

Federated Breast Cancer Detection Enhanced by Synthetic Ultrasound Image Augmentation

Hongyi Pan
Department of Radiology
Northwestern University
Chicago, Illinois, USA
hongyi.pan@northwestern.edu

Ziliang Hong
Departments of BME and Radiology
Northwestern University
Chicago, Illinois, USA
ZiliangHong2029@u.northwestern.edu

Gorkem Durak
Department of Radiology
Northwestern University
Chicago, Illinois, USA
gorkem.durak@northwestern.edu

Ziyue Xu
NVIDIA
Bethesda, MD, USA
ziyuex@nvidia.com

Ulas Bagci
Departments of Radiology
Northwestern University
Chicago, Illinois, USA
ulas.bagci@northwestern.edu

Abstract—Federated learning (FL) has emerged as a promising paradigm for collaboratively training deep learning models across institutions without exchanging sensitive medical data. However, its effectiveness is often hindered by limited data availability and non-independent, identically distributed data across participating clients, which can degrade model performance and generalization. To address these challenges, we propose a generative AI based data augmentation framework that integrates synthetic image sharing into the federated training process for breast cancer diagnosis via ultrasound images. Specifically, we train two simple class-specific Deep Convolutional Generative Adversarial Networks: one for benign and one for malignant lesions. We then simulate a realistic FL setting using three publicly available breast ultrasound image datasets: BUSI, BUS-BRA, and UDIAT. FedAvg and FedProx are adopted as baseline FL algorithms. Experimental results show that incorporating a suitable number of synthetic images improved the average AUC from 0.9206 to 0.9237 for FedAvg and from 0.9429 to 0.9538 for FedProx. We also note that excessive use of synthetic data reduced performance, underscoring the importance of maintaining a balanced ratio of real and synthetic samples. Our findings highlight the potential of generative AI based data augmentation to enhance FL results in the breast ultrasound image classification task.

Index Terms—Federated Learning, Breast Ultrasound, DCGAN, Synthetic Data, Medical Image Classification.

I. INTRODUCTION

Breast cancer is the most prevalent type of cancer and one of the leading causes of cancer-related deaths among women [1]. Approximately 13% of the female population in the United States is projected to receive a breast cancer diagnosis at some point in their lives [2], and more than 300,000 women are expected to be diagnosed with invasive breast cancer each year [3]. Recently, deep learning techniques have achieved remarkable success in automating breast ultrasound image classification [4]–[6] and segmentation [7]–[9] tasks. However, training robust and generalizable models typically requires large-scale, diverse datasets that are often challenging to obtain due to privacy regulations and data-sharing restrictions across medical institutions.

Generative Adversarial Networks (GANs) [10] have become a powerful tool for medical image synthesis, particularly in settings

with limited annotated data. The original or “vanilla” GAN architecture has inspired a range of more stable and expressive variants tailored to different applications. Deep Convolutional GANs (DCGANs) [11]–[13] introduced convolutional layers to improve training stability and output quality, and have been widely adopted for medical image augmentation tasks across modalities. StyleGAN [14] further enhanced image fidelity and control over synthesis through its style-based generator, and has been adapted to generate high-resolution images. These GAN-based methods have shown significant promise in generating diverse and realistic samples to augment training data or simulate rare conditions. More recently, diffusion probabilistic models [13], [15]–[18] have emerged as a compelling alternative due to their superior sample diversity and stability. However, their slow sampling speed and high computational demands limit their practicality in time-sensitive or resource-constrained settings such as federated learning. In this work, we adopt simple, hence practical, DCGANs for their balance of efficiency and effectiveness so that it can be translated into clinical evaluation more easily than other alternatives, such as flow based or diffusion based algorithms. We also acknowledge that our approach can further be extended to more advanced generative models.

Federated learning enables collaborative model training across multiple institutions while preserving data privacy by avoiding direct data sharing [19]–[26]. Challenges such as non-IID data distribution, domain shifts, and limited local data hamper federated learning performance. Recent works have explored personalized federated learning [27] and domain generalization [28]–[31] to mitigate these issues. In this work, we integrate synthetic data generation within federated learning to enhance breast ultrasound classification under realistic multi-center heterogeneity.

To this end, we propose a federated learning framework that incorporates class-specific DCGANs [11] to generate synthetic breast ultrasound images for data augmentation across clients. By centrally training separate GAN models for *benign* and *malignant* cases and distributing the synthetic images in a privacy-preserving manner, our approach addresses critical challenges of data scarcity, domain heterogeneity, and privacy protection inherent in multi-institutional medical imaging. Extensive experiments on three publicly available datasets (BUS-BRA [32], BUSI [33], and UDIAT [34]) demonstrate that introducing a suitable amount of synthetic images consistently improves classification performance, increasing FedAvg’s average AUC from 0.9206 to 0.9237 and FedProx’s from 0.9429 to 0.9538. However, our ablation study reveals that excessive synthetic data can degrade both accuracy and AUC, underscoring the importance

This work was supported by the following NIH grants: NCI R01-CA246704, R01-CA240639, U01-CA268808, and NHLBI R01-HL171376.

of carefully balancing real and synthetic samples to enhance model generalization while preserving data privacy.

II. METHODOLOGY

A. Problem Statement

Given breast ultrasound datasets distributed across multiple clinical centers, our goal is to collaboratively train a binary classification model to distinguish benign from malignant lesions under the federated learning setting. Let there be K clients, each with a local dataset $\mathcal{D}_K = \{(x_0^k, y_0^k), \dots, (x_{n_k-1}^k, y_{n_k-1}^k)\}$, where x_i^k is a BUS image and y_i^k is the corresponding label (0 for benign, 1 for malignant). In standard FL, the global model f_θ is optimized by minimizing the weighted sum of local losses without exchanging raw data:

$$\min_{\theta} \sum_{k=0}^{K-1} \frac{n_k}{n} \mathcal{L}_k(\theta), \quad (1)$$

where

$$\mathcal{L}_k(\theta) = \frac{1}{n_k} \sum_{i=0}^{n_k-1} \ell(f_\theta(x_i^k), y_i^k). \quad (2)$$

Here, $\ell(\cdot)$ denotes the binary cross-entropy loss, and $n = \sum_{k=1}^K n_k$ is the total number of samples. However, this setup faces practical challenges such as non-IID data distributions across clients, limited local data (especially malignant cases), and poor generalization.

B. Synthetic breast ultrasound images generation via DCGAN

To address the challenges of data scarcity and non-IID distributions in federated breast ultrasound classification, we incorporate synthetic image generation using DCGANs [11]. GAN-based data augmentation has shown promise in medical imaging for enriching training sets with realistic, domain-relevant variations [35]. In this work, we do not use diffusion models because, despite their recent success in producing high-quality and diverse images, they are computationally intensive and exhibit slow sampling speeds. Specifically, we train two separate DCGAN models: one for generating benign images and one for malignant images. Both models are trained centrally using the combined training and validation datasets while strictly excluding all test data to prevent data leakage. The generator network maps a random noise vector concatenated with a lesion mask to a grayscale BUS image, aiming to produce realistic ultrasound textures while maintaining anatomical plausibility. The discriminator learns to differentiate between real and synthetic images, enforcing the realism of generated outputs.

Formally, let $z \sim \mathcal{N}(0, I)$ be the latent noise vector and M be a binary lesion mask. The generator $G(z, M)$ outputs a synthetic ultrasound image I_{syn} , while the discriminator D attempts to distinguish real images I_{real} from I_{syn} . The objective functions for G and D follow the standard DCGAN formulation:

$$\min_G \max_D \mathbb{E}_{\mathbf{x} \sim p_{data}(\mathbf{x})} [\log D(\mathbf{x})] + \mathbb{E}_{\mathbf{z} \sim p_z(\mathbf{z})} [\log(1 - D(G(\mathbf{z})))] \quad (3)$$

Fig. 1 illustrates the architecture of the DCGAN employed in this study. The generator network produces a 128×128 synthetic breast ultrasound image from a 128-dimensional latent noise vector using six 2D transposed convolutional layers. The discriminator, composed of six 2D convolutional layers, classifies input images as real or synthetic. We also experimented with generating 256×256 images using a similarly scaled architecture, but observed unstable training and poor convergence. As a result, we generate images at a resolution of 128×128 , which are subsequently upsampled to 224×224 before being used for training the classification networks.

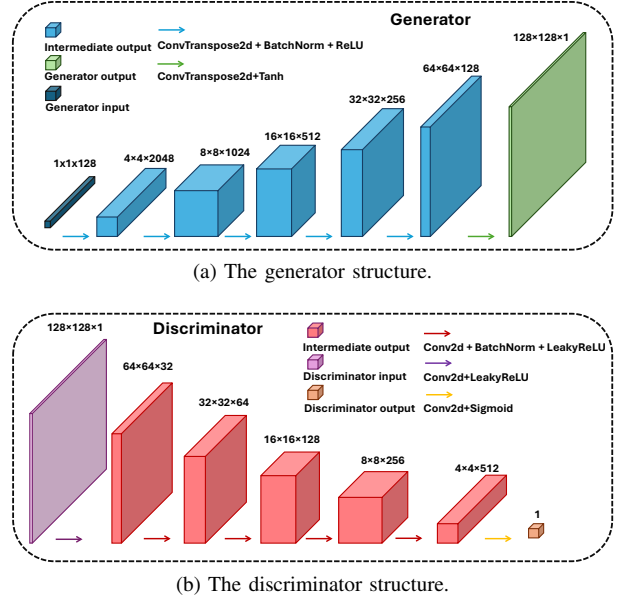


Fig. 1: Architecture of the class-specific DCGAN used for generating synthetic breast ultrasound images. Two pairs of models are trained for benign and malignant cases, respectively, and each consists of a generator and a discriminator with symmetric convolutional and transposed convolutional layers.

C. Federated Learning with Synthetic Images

To evaluate the utility of synthetic breast ultrasound images in privacy-preserving distributed training, we simulate a federated learning setup where synthetic images are shared across multiple clients. Each client hosts a subset of real BUS images from one dataset, reflecting data heterogeneity across imaging centers. Synthetic images generated by DCGAN are centrally produced and distributed identically to all clients to serve as shared prior knowledge. These synthetic samples help mitigate data imbalance and enhance generalization across clients.

In this work, we adopt two widely-used federated learning algorithms as baselines: FedAvg [19] and FedProx [20]. Both algorithms operate under the standard federated learning protocol: at each communication round, a global model is distributed to all clients, which perform local updates using their data, followed by aggregation at the server. In detail:

- FedAvg [19] performs simple weighted averaging of the local model updates:

$$\mathbf{w}^{t+1} = \sum_{k=0}^{K-1} \frac{n_k}{n} \mathbf{w}_k^t, \quad (4)$$

where w_k^t is the model from client k , n_k is the number of samples at client k , and $n = \sum_{k=0}^{K-1} n_k$.

- FedProx [20] introduces a proximal term to stabilize training across heterogeneous data:

$$\min_{\mathbf{w}} f_k(\mathbf{w}) + \frac{\mu}{2} \|\mathbf{w} - \mathbf{w}^t\|^2, \quad (5)$$

where μ controls the strength of the proximal regularization toward the global model \mathbf{w}^t .

In our study, each client performs multiple local updates using a mix of real and synthetic breast ultrasound images. The synthetic data provides regularization and prevents overfitting to local client-specific

Algorithm 1 Federated learning with synthetic images.

Input: Global model initial wights \mathbf{w}^0 , training datasets \mathcal{D}_K with the corresponding length n_k for $k = 0, 1, \dots, K - 1$, synthetic datasets \mathcal{S} .

Hyperparameters: number of epochs T , adaptive aggregation weights step size s .

Output: Well-trained global model wights \mathbf{w}^T .

- 1: $n = \sum_{k=0}^{K-1} n_k$;
 - 2: **for** $t = 0, 1, \dots, T - 1$ **do**
 - 3: Update \mathbf{w}^t on \mathcal{S} ;
 - 4: **for** $k = 0, 1, \dots, K - 1$ **do**
 - 5: Assign weights to local model: $\mathbf{w}_k^t = \mathbf{w}^t$;
 - 6: Update \mathbf{w}_k^t using \mathcal{D}_k ;
 - 7: **end for**
 - 8: Aggregate models: $\mathbf{w}^{t+1} = \sum_{k=0}^{K-1} \frac{n_k}{n} \mathbf{w}_k^t$;
 - 9: **end for**
-

distributions, thereby improving global model generalizability. We evaluate both centralized and federated settings to quantify the benefit of incorporating synthetic data in federated breast ultrasound classification.

III. EXPERIMENTS

A. Dataset Description

We leverage three publicly available breast ultrasound datasets to conduct federated learning experiments for binary classification of benign versus malignant lesions:

- BUS-BRA [32]: The BUS-BRA dataset is a publicly available collection of breast ultrasound images, released in 2023, and acquired from 1,064 female patients at the National Institute of Cancer in Rio de Janeiro, Brazil. It comprises 1,875 anonymized B-mode ultrasound images in PNG format, collected using four different ultrasound scanners during routine clinical examinations. Each image is annotated with biopsy-proven diagnostic labels (benign or malignant), BI-RADS categories (ranging from 2 to 5), and expert-delineated lesion segmentation masks. 1,268 benign and 607 malignant images are utilized for the binary classification task in this study.
- BUSI [33]: The Breast Ultrasound Images (BUSI) dataset was collected in 2018 at Baheya Hospital in Egypt and contains ultrasound scans from 600 female patients aged between 25 and 75 years. The dataset includes a total of 780 B-mode ultrasound images in PNG format, with an average resolution of 500×500 pixels. Each image is annotated with a corresponding binary mask delineating the lesion area. The BUSI dataset is categorized into three diagnostic classes: 133 normal, 437 benign, and 210 malignant images. However, since the other datasets used in this study do not include normal cases, only the benign and malignant samples are retained from BUSI for consistency in the binary classification task in this study.
- UDIAT [34]: The UDIAT dataset was collected in 2012 at the UDIAT Diagnostic Centre of the Parc Taulí Corporation in Sabadell, Spain. It comprises 163 B-mode breast ultrasound images acquired using a Siemens ACUSON Sequoia C512 system with a 17L5 HD linear array transducer operating at 8.5 MHz. The mean resolution of the images is approximately 760×570 pixels. Each image contains one or more breast lesions, and all lesions were manually delineated by experienced radiologists. The dataset includes 109 benign and 54 malignant cases, with benign lesions consisting primarily of cysts and fibroadenomas, and malignant cases including invasive ductal carcinoma, ductal carcinoma in situ, and other malignancies. All

TABLE I: Dataset Description.

Dataset	Benign	Malignant	Total
BUS-BRA	1268	607	1875
BUSI	437	210	647
UDIAT	109	54	163

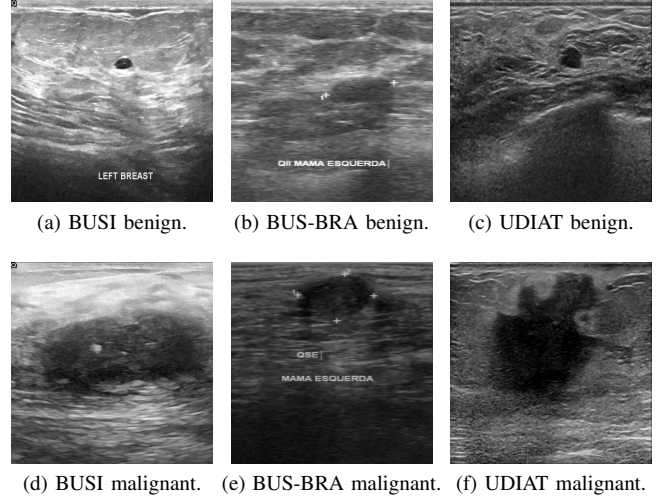


Fig. 2: Breast ultrasound image samples from the BUSI, BUS-BRA, and UDIAT datasets.

images and corresponding lesion masks are publicly available for research purposes.

Samples of the breast ultrasound images are visualized in Fig 2, and the characteristics of the datasets are summarized in Table I. For each dataset, we split the images into training, validation, and testing subsets using an approximate ratio of 3:1:2, ensuring that both benign and malignant cases are proportionally represented across splits. The training and validation subsets are used for both classification model training and DCGAN-based synthetic image generation. Importantly, no testing images are used during DCGAN training to preserve the integrity of the evaluation and avoid data leakage.

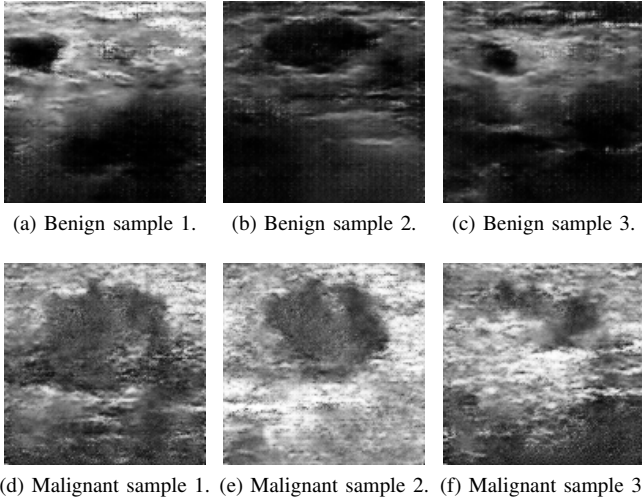
B. Implementation Details

All experiments were implemented in Python using the PyTorch framework and executed on a workstation equipped with an NVIDIA RTX 3090 GPU. For synthetic image generation, two separate DCGAN models were trained using the combined training and validation data from all three datasets—one model for benign cases and the other for malignant cases. Both the generator and discriminator followed the DCGAN architecture illustrated in Fig. 1. Each model was trained for 500 epochs using the Adam optimizer [36] with a learning rate of 0.0002 and a batch size of 128. After training, 1,000 synthetic benign and 1,000 synthetic malignant images were generated and uniformly distributed to all clients for data augmentation during federated training. Representative examples of the generated synthetic images are shown in Fig. 3.

For the classification task, we utilized ImageNet-pretrained DenseNet-121 [37] as the backbone model. The federated learning setup simulated three clients (BUS-BRA, BUSI, and UDIAT datasets). We adapt FedAvg and FedProx as baseline federated learning algorithms. At each communication round, the global model was distributed to all clients, where each performs local training for one epoch with a batch size of 32 using the AdamW optimizer [38]. The initial learning rate was set to 0.001 and decayed by a factor

TABLE II: Federated breast ultrasound image classification performance with and without synthetic image augmentation. Models are evaluated on the test set using the checkpoints that achieved the highest average AUC on the validation data.

Method	Accuracy			Average	AUC			Average
	BUSBRA	BUSI	UDIAT		BUSBRA	BUSI	UDIAT	
Centralized Learning	0.8507	0.9000	0.9394	0.8967	0.9199	0.9510	0.9463	0.9391
FedAvg	0.8480	0.8923	0.8788	0.8730	0.9191	0.9048	0.9380	0.9206
FedAvg+Synthetic	0.8773	0.8615	0.9394	0.8928	0.9373	0.9164	0.9174	0.9237
FedProx	0.8747	0.8923	0.9394	0.9021	0.9318	0.9424	0.9545	0.9429
FedProx+Synthetic	0.8720	0.9077	0.9091	0.8963	0.9454	0.9532	0.9628	0.9538



(d) Malignant sample 1. (e) Malignant sample 2. (f) Malignant sample 3.

Fig. 3: Synthetic breast ultrasound images generated by class-specific DCGANs. These images are used to augment local training data in the federated learning framework.

of 10 every 30 epochs. For FedProx, the proximal term coefficient was set to $\mu = 0.03$. After local training, models were aggregated at the server using weighted averaging proportional to the number of training samples at each client. To prevent overfitting on synthetic data, the initial learning rate for synthetic image batches was set to 0.0001 and decayed by a factor of 10 every 30 epochs. In each epoch, we randomly selected 160 synthetic images (5 batches) for training, ensuring that synthetic data comprised approximately 12% of each client’s training data. In the ablation study, we observed that using too many synthetic images can negatively impact model performance, highlighting the importance of careful balancing between real and synthetic data. The entire training process was conducted for 100 communication rounds, and the global model achieving the highest average AUC across validation sets was selected for final evaluation on the test set.

C. Federated Breast Ultrasound Image Classification Results and Ablation Study

Table II presents the quantitative results of the federated breast ultrasound image classification experiments. The introduction of synthetic images during federated training led to performance improvements for both FedAvg and FedProx. Specifically, the average AUC for FedAvg increased from 0.9206 to 0.9237, while FedProx achieved a more substantial improvement, with the average AUC rising from 0.9429 to 0.9538. For reference, the centralized learning model trained on the combined dataset achieved an AUC of 0.9391, indicating that the proposed federated framework with synthetic augmentation (especially FedProx) can match or even outperform centralized training while preserving data privacy. These results demonstrated that augmenting client datasets with centrally generated synthetic images improved classification performance in a privacy-preserving federated learning setting.

We then conducted an ablation study to investigate the impact of introducing a larger volume of synthetic images during training. These results are visualized as “FedAvg+Synthetic (heavy)” in Fig. 4. Unlike the baseline synthetic image usage setting, the excessive inclusion of synthetic data led to a noticeable drop in both accuracy (ACC) and area under the curve (AUC). This performance degradation was likely due to the synthetic images introducing distributional noise, which may have diluted the informative patterns in the real data. This finding highlights the importance of carefully balancing synthetic and real data when using generative augmentation in federated learning.

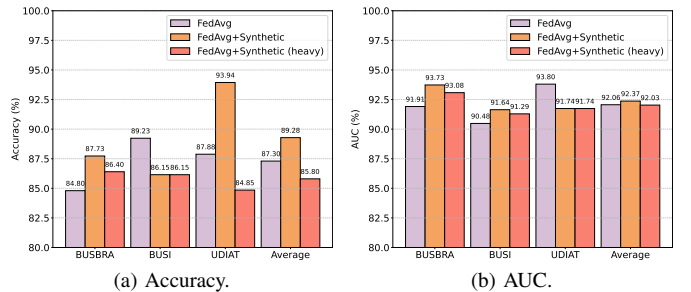


Fig. 4: Ablation study results showing the effect of increasing the number of synthetic images during federated training. While moderate augmentation improves performance, excessive synthetic data leads to a decline in both AUC and accuracy, highlighting the importance of balancing real and synthetic samples.

These experiments demonstrated that a suitable amount of synthetic image augmentation improved federated classification performance, while excessive use of synthetic data led to decreased AUC and accuracy, underscoring the importance of balanced synthetic integration.

IV. CONCLUSION

In this work, we developed a federated learning framework for breast ultrasound image classification augmented with class-specific synthetic images generated by DCGANs. Using three publicly available BUS datasets (BUSI, BUS-BRA, and UDIAT), we simulated a realistic multi-center FL setup and assessed the impact of synthetic augmentation. Our results demonstrated that incorporating a suitable amount of synthetic images improved model performance: FedAvg’s average AUC increased from 0.9206 to 0.9237, and FedProx improved from 0.9429 to 0.9538. However, excessive use of synthetic data caused a decline in both AUC and accuracy, indicating that over-regularization or domain shift from synthetic images may negatively affect generalization. These findings suggest that while generative augmentation holds promise for enhancing federated medical imaging models, careful calibration of synthetic-to-real data ratios is critical for maximizing benefit. Although our current framework employs DCGANs for efficiency, future work could explore integrating diffusion-based generative models to potentially improve synthetic image quality and diversity.

REFERENCES

- [1] Sergiusz Łukasiewicz, Marcin Czezelewski, Alicja Forma, Jacek Baj, Robert Sitarz, and Andrzej Stanislawek. Breast cancer—epidemiology, risk factors, classification, prognostic markers, and current treatment strategies—an updated review. *Cancers*, 13(17):4287, 2021.
- [2] LAG Ries, D Melbert, M Krapcho, DG Stinchcomb, N Howlander, MJ Horner, A Mariotto, BA Miller, EJ Feuer, SF Altekruse, et al. *Seer cancer statistics review, 1975–2005*. Bethesda, MD: National Cancer Institute, 2999, 2008.
- [3] Harnoor Singh and Nilan Bhakta. Minimally invasive breast cancer: how to find early breast cancers. *Current Breast Cancer Reports*, 16(2):117–125, 2024.
- [4] Mohammad I Daoud, Samir Abdel-Rahman, and Rami Alazrai. Breast ultrasound image classification using a pre-trained convolutional neural network. In *2019 15th International Conference on Signal-Image Technology & Internet-Based Systems (SITIS)*, pages 167–171. IEEE, 2019.
- [5] Fatemeh Taheri and Kambiz Rahbar. Improving breast cancer classification in fine-grain ultrasound images through feature discrimination and a transfer learning approach. *Biomedical Signal Processing and Control*, 106:107690, 2025.
- [6] Jaber Qezelbash-Chamak and Karen Hicklin. A hybrid learnable fusion of convnext and swin transformer for optimized image classification. *IoT*, 6(2):30, 2025.
- [7] Qiqi He, Qiuju Yang, and Minghao Xie. Hctnet: A hybrid cnn-transformer network for breast ultrasound image segmentation. *Computers in Biology and Medicine*, 155:106629, 2023.
- [8] Huaikun Zhang, Jing Lian, and Yide Ma. Fet-unet: Merging cnn and transformer architectures for superior breast ultrasound image segmentation. *Physica Medica*, 133:104969, 2025.
- [9] Teng Wang, Jun Liu, and Jinshan Tang. A cross-scale attention-based u-net for breast ultrasound image segmentation. *Journal of Imaging Informatics in Medicine*, pages 1–14, 2025.
- [10] Ian J Goodfellow, Jean Pouget-Abadie, Mehdi Mirza, Bing Xu, David Warde-Farley, Sherjil Ozair, Aaron Courville, and Yoshua Bengio. Generative adversarial nets. *Advances in neural information processing systems*, 27, 2014.
- [11] Alec Radford, Luke Metz, and Soumith Chintala. Unsupervised representation learning with deep convolutional generative adversarial networks. *arXiv preprint arXiv:1511.06434*, 2015.
- [12] Tomoyuki Fujioka, Mio Mori, Kazunori Kubota, Yuka Kikuchi, Leona Katsuta, Mio Adachi, Goshi Oda, Tsuyoshi Nakagawa, Yoshio Kitazume, and Ukihide Tateishi. Breast ultrasound image synthesis using deep convolutional generative adversarial networks. *Diagnostics*, 9(4):176, 2019.
- [13] Yasamin Medghalchi, Niloufar Zakariaei, Arman Rahmim, and Ilker Hacıhaliloğlu. Synthetic vs. classic data augmentation: Impacts on breast ultrasound image classification. *IEEE Transactions on Ultrasonics, Ferroelectrics, and Frequency Control*, 2025.
- [14] Tero Karras, Samuli Laine, and Timo Aila. A style-based generator architecture for generative adversarial networks. In *Proceedings of the IEEE/CVF conference on computer vision and pattern recognition*, pages 4401–4410, 2019.
- [15] Jonathan Ho, Ajay Jain, and Pieter Abbeel. Denoising diffusion probabilistic models. *Advances in neural information processing systems*, 33:6840–6851, 2020.
- [16] Robin Rombach, Andreas Blattmann, Dominik Lorenz, Patrick Esser, and Björn Ommer. High-resolution image synthesis with latent diffusion models. In *Proceedings of the IEEE/CVF conference on computer vision and pattern recognition*, pages 10684–10695, 2022.
- [17] Lvmin Zhang, Anyi Rao, and Maneesh Agrawala. Adding conditional control to text-to-image diffusion models. In *Proceedings of the IEEE/CVF international conference on computer vision*, pages 3836–3847, 2023.
- [18] Zheyuan Zhang, Lanhong Yao, Bin Wang, Debesh Jha, Gorkem Durak, Elif Keles, Alpay Medetalibeyoglu, and Ulas Bagci. Diffboost: Enhancing medical image segmentation via text-guided diffusion model. *IEEE Transactions on Medical Imaging*, 2024.
- [19] Brendan McMahan, Eider Moore, Daniel Ramage, Seth Hampson, and Blaise Agüera y Arcas. Communication-efficient learning of deep networks from decentralized data. In *Artificial intelligence and statistics*, pages 1273–1282. PMLR, 2017.
- [20] Tian Li, Anit Kumar Sahu, Manzil Zaheer, Maziar Sanjabi, Ameet Talwalkar, and Virginia Smith. Federated optimization in heterogeneous networks. *Proceedings of Machine learning and systems*, 2:429–450, 2020.
- [21] Xiaoxiao Li, Meirui Jiang, Xiaofei Zhang, Michael Kamp, and Qi Dou. Fedbn: Federated learning on non-iid features via local batch normalization. *arXiv preprint arXiv:2102.07623*, 2021.
- [22] Runxuan Miao and Erdem Koyuncu. Federated momentum contrastive clustering. *ACM Transactions on Intelligent Systems and Technology*, 15(4):1–19, 2024.
- [23] Peyman Gholami and Hulya Seferoglu. Digest: Fast and communication efficient decentralized learning with local updates. *IEEE Transactions on Machine Learning in Communications and Networking*, 2:1456–1474, 2024.
- [24] Hongyi Pan, Gorkem Durak, Zheyuan Zhang, Yavuz Taktak, Elif Keles, Halil Ertugrul Aktas, Alpay Medetalibeyoglu, Yury Velichko, Concetto Spampinato, Ivo Schoots, et al. Adaptive aggregation weights for federated segmentation of pancreas mri. *arXiv preprint arXiv:2410.22530*, 2024.
- [25] Hongyi Pan, Ziliang Hong, Gorkem Durak, Elif Keles, Halil Ertugrul Aktas, Yavuz Taktak, Alpay Medetalibeyoglu, Zheyuan Zhang, Yury Velichko, Concetto Spampinato, et al. Ipmn risk assessment under federated learning paradigm. *arXiv preprint arXiv:2411.05697*, 2024.
- [26] Yipu Zhang, Likai Wang, Kuan-Jui Su, Aiyong Zhang, Hao Zhu, Xiaowen Liu, Hui Shen, Vince D Calhoun, Yuping Wang, and Hongwen Deng. A privacy-preserving domain adversarial federated learning for multi-site brain functional connectivity analysis. *arXiv preprint arXiv:2502.01885*, 2025.
- [27] Alysa Ziyang Tan, Han Yu, Lizhen Cui, and Qiang Yang. Towards personalized federated learning. *IEEE transactions on neural networks and learning systems*, 34(12):9587–9603, 2022.
- [28] Quande Liu, Cheng Chen, Jing Qin, Qi Dou, and Pheng-Ann Heng. Fedgd: Federated domain generalization on medical image segmentation via episodic learning in continuous frequency space. In *Proceedings of the IEEE/CVF conference on computer vision and pattern recognition*, pages 1013–1023, 2021.
- [29] Ruipeng Zhang, Qinwei Xu, Jiangchao Yao, Ya Zhang, Qi Tian, and Yanfeng Wang. Federated domain generalization with generalization adjustment. In *Proceedings of the IEEE/CVF Conference on Computer Vision and Pattern Recognition*, pages 3954–3963, 2023.
- [30] Hongyi Pan, Bin Wang, Zheyuan Zhang, Xin Zhu, Debesh Jha, Ahmet Enis Cetin, Concetto Spampinato, and Ulas Bagci. Domain generalization with fourier transform and soft thresholding. In *ICASSP 2024-2024 IEEE International Conference on Acoustics, Speech and Signal Processing (ICASSP)*, pages 2106–2110. IEEE, 2024.
- [31] Hongyi Pan, Debesh Jha, Koushik Biswas, and Ulas Bagci. Frequency-based federated domain generalization for polyp segmentation. *arXiv preprint arXiv:2410.02044*, 2024.
- [32] Wilfrido Gómez-Flores, Maria Julia Gregorio-Calas, and Wagner Coelho de Albuquerque Pereira. Bus-bra: a breast ultrasound dataset for assessing computer-aided diagnosis systems. *Medical Physics*, 51(4):3110–3123, 2024.
- [33] Walid Al-Dhabyani, Mohammed Goma, Hussien Khaled, and Aly Fahmy. Dataset of breast ultrasound images. *Data in brief*, 28:104863, 2020.
- [34] Moi Hoon Yap, Gerard Pons, Joan Marti, Sergi Ganau, Melcior Sentis, Reyer Zwiggelaar, Adrian K Davison, and Robert Marti. Automated breast ultrasound lesions detection using convolutional neural networks. *IEEE journal of biomedical and health informatics*, 22(4):1218–1226, 2017.
- [35] Ismail Irmakci, Zeki Emre Unel, Nazli İkizler-Cinbis, and Ulas Bagci. Multi-contrast mri segmentation trained on synthetic images. In *2022 44th Annual International Conference of the IEEE Engineering in Medicine & Biology Society (EMBC)*, pages 5030–5034. IEEE, 2022.
- [36] Diederik P Kingma and Jimmy Ba. Adam: A method for stochastic optimization. *arXiv preprint arXiv:1412.6980*, 2014.
- [37] Gao Huang, Zhuang Liu, Laurens Van Der Maaten, and Kilian Q Weinberger. Densely connected convolutional networks. In *Proceedings of the IEEE conference on computer vision and pattern recognition*, pages 4700–4708, 2017.
- [38] Ilya Loshchilov and Frank Hutter. Decoupled weight decay regularization. *arXiv preprint arXiv:1711.05101*, 2017.